

## MICROSTRUCTURE AND CHEMICAL CHARACTERIZATION OF *RAPANA THOMASIANA* SHELL

Viviana SEREANU<sup>1</sup>, Daniela-Laura FERARU<sup>2</sup>, Georgeta PREDEANU<sup>3</sup>, Aurelia MEGHEA<sup>4</sup>

*In the present study, the exoskeleton of *Rapana thomasiana*, better known as *Rapna venosa*, collected from the Romanian Black Sea coast (Midia Cape and Limanu) has been characterized based on physical-chemical and morpho-structural analyses. Few data were found in literature regarding rapana shell structure and chemical characterization. Therefore, firstly, the gastropods' shell microstructure was determined by both optical and scanning electron microscopy (SEM). The optical microscopy observations point out that the shell of rapana is characterized by three main layers, an amorphous combined with a crossed lamellar prismatic outer shell layer, an intermediate simple prismatic layer and a lamello - fibrillar layer inwards, as further characterized by SEM observations. The aim of this study is to determine if there are differences in terms of mineral and chemical composition among the exoskeletons' layers. For this purpose, the mineral content of each layer was further analyzed using X-ray fluorescence spectroscopy. Infrared spectroscopy allowed to estimate the relative content of polymorphic forms of calcite, which was in agreement with the water salinity in the sampling sites.*

**Keywords:** *Rapana thomasiana*, *Rapana venosa*, shell chemical characterization, exoskeleton microstructure

### 1. Introduction

*Rapana venosa* (Valenciennes, 1846) or *Rapana thomasiana* (Crosse, 1861) is a muricid gastropod, originating from the Sea of Japan and occurring in abundance into the Black Sea [1, 2]. *Rapana venosa* belongs to the phylum Mollusca, class Gastropoda, and was recently re-classified from the subclass Prosobranchia into the subclass Orthogastropoda, family Muricidae, subfamily Rapaninae (subfamily Thaididae) [3]. This mollusk is a predatory gastropod,

<sup>1</sup> PhD student, Faculty of Applied Chemistry and Material Science, University POLITEHNICA of Bucharest, Romania, e-mail: vivianasereanu@gmail.com

<sup>2</sup> PhD chem., Physical-Chemical Examination Department–National Forensic Science Institute – General Inspectorate of Romanian Police, Bucharest, Romania, e-mail: danielaferaru@yahoo.com

<sup>3</sup> PhD eng., Research Centre for Environmental Protection and Ecological Technologies, University POLITEHNICA of Bucharest, Romania, e-mail: gpredeanu@gmail.com

<sup>4</sup> Prof., Dep. of Inorganic Chemistry, Physical Chemistry and Electrochemistry, University POLITEHNICA of Bucharest, Romania, e-mail: a.meghea@gmail.com

which is considered an environmental threat for bivalves of economic interest [4, 5].

Boggild (1930) was the pioneer in describing and classifying from mineralogical, crystallographic and microstructural points of view the main molluscan shell structure. He described nacre as the inner iridescent layer which is commonly found in the molluscan classes of Gastropoda, Bivalvia and Cephalopoda [6]. Petitjean reported on the structural, mineralogical and chemical characteristics of the Muricids and recognized a calcitic "cortex" and an aragonitic "ostracum" in various species. He assigned the presence of the calcitic cortex as a subfamily taxonomic characteristic for the Rapaninae subfamily [7]. Recently, Kiel continues the study of the gastropods' shell structure by electron microscopically investigation of 24 gastropod species, but not including *Rapana venosa* in his study [8]. Further microscopy studies were directed towards other species and therefore an independent and accurate study of *Rapana venosa* shell microstructure was difficult to find.

Morphology studies of this species proved that local variation may occur in morphometry and coloration depending on benthic substrate [9-12]. The chemical analysis of rapana shell composition done by Jitar et al. [13], as well as our previous results [14] identified that concentrations of minerals in rapana exoskeleton, differ among regions of the Romanian coast of the Black Sea accordingly to the environment and seawater pollution level. In sediments, due to the influence of anthropogenic pollution represented by the municipal wastewater treatment plant, as well as by the harbor wastewater, at Constanța South, in the harbor area, as well as in Mangalia, were registered higher mean values for some heavy metals (Cu, Ni, Cr, Cd, Pb). Lower concentrations of heavy metals with few significant differences revealed marine sediments sampled from Constanta North, Eforie South, Costinesti and Vama Veche [13]. However, even though previous studies were conducted using adequate analytical chemistry techniques (atomic absorption spectrometry and inductively coupled plasma spectrometry) a few data are available on the structure and composition of the shell of *Rapana thomasiana*.

The aim of this paper is to study the microstructure and chemical composition of the shell of gastropod *Rapana thomasiana* by using optical and electron microscopy (SEM), X-ray fluorescence spectroscopy (XRF) and infrared spectroscopy (FTIR) analyses. Moreover, a detailed study was carried out in order to establish if there are differences in terms of mineral composition among the exoskeletons' layers. For this purpose, the mineral content of each layer was further analyzed.

## 2. Materials and Methods

Stranded adult individuals of *Rapana thomasiana* were sampled from two locations along the coast of the Romanian Black Sea: Midia Cape (N44.34507°, E28.69201°) located approximately 100 km to the South of the Danube River, and near the Rompetrol refinery; the second sampling site was the wild beach of Limanu (N43.77230°, E28.57922°), located near 2 Mai village at the South of Mangalia harbour.

### 2.1. Optical microscopy

Fractured longitudinal and transversal sections of rapana shells were prepared for microstructure and chemical analysis (Fig. 1A). The particulate blocks for microscopically analysis were ground down using progressively finer wet carborundum papers; the final grind was 1200 wet paper; final polishing of the pellets was done using colloidal suspension of aluminium oxide or diamond powder of 3.00  $\mu\text{m}$  and  $<1.00\ \mu\text{m}$  grain size. The surface was then lightly etched in 5% formic acid for 15 s to reveal microtextural details within the samples (e.g. different layers). The analyses were performed using a reflected white light (RL) binocular optical microscope Olympus BX51M equipped with a 12 V, 100 W halogen lamp, polarizer, analyser with a rotation of 360°, oil immersion objectives, and a combined magnification of  $\times 500$ , coupled with a transmission images camera model CCD-1300QB for image collection. First insights were obtained by observing sections of longitudinal and transversal planes of shell ridges, with both normal and crossed nicols.

### 2.2. Scanning electron microscopy (SEM)

SEM observation of the rapana microstructure was carried out on both fractured and polished sections of the shell. Samples were observed intact using a JEOL JSM 6480LV Microscope, accelerating voltage 20 kV, magnification 30-650x, pressure 16 Pa, equipped with Si/Li X-ray detector.

### 2.3. X-ray fluorescence spectroscopy (XRF)

Elemental composition of *Rapana thomasiana* exoskeleton from Midia Cape and Limanu was analyzed using X-ray fluorescence spectrometry. The analyses were made both on fractured and polished sections of the shell. Measurements were performed with Si/Li X-ray detector attached to the JEOL JSM 6480LV Microscope. Three measurements were done for each magnification at 2 mm, 200  $\mu\text{m}$  and 90  $\mu\text{m}$  for the exterior and internal surfaces of the shell, as well as for each of the three main layers of rapana skeleton. An arithmetic mean of the registered values for each analyzed part of the shell was done using the software Microsoft Excel 2010.

Since each element present in a sample produces a set of characteristic fluorescent X-rays (“a fingerprint”) unique for that specific element, XRF spectroscopy is an excellent technique for qualitative and quantitative analysis of material composition.

#### 2.4. Infrared spectroscopy (FTIR)

To highlight the characteristic covalent bonds of functional groups existing in the composition of rapana shell, infrared spectra have been studied for all the samples, and then analyzed by transmission, using a spectrometer FT-IR type Tensor 27 equipped with a reflection Golden Gate ATR crystal diamond, provided by Bruker. Infrared spectrum was recorded for each sample between  $400\text{ cm}^{-1}$  and  $4000\text{ cm}^{-1}$ .

### 3. Results and Discussion

#### 3.1. Microstructure

Thin sections show that the shell (Fig. 1A) is composed of three main layers (Fig. 1 B–D): an amorphous outer shell layer, an intermediate crossed lamellar layer and an inner shell layer or nacre.

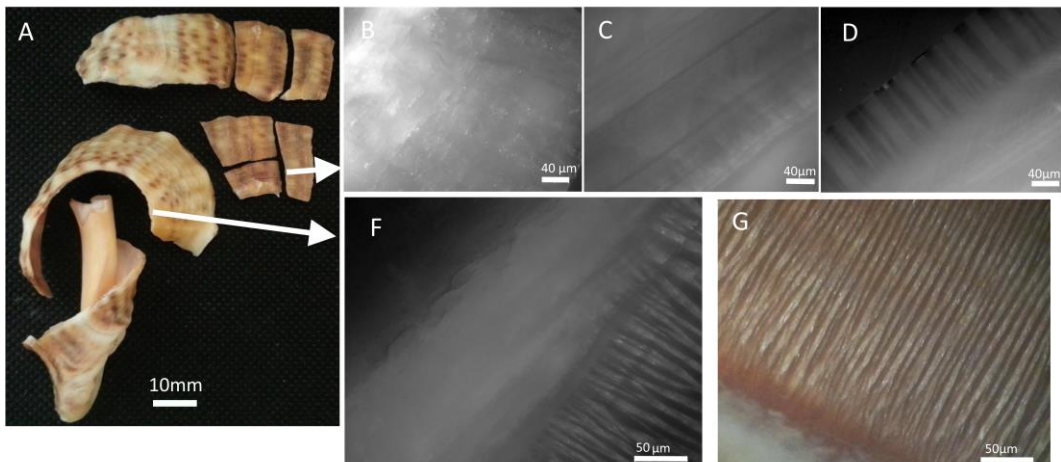


Fig. 1. Photomicrographs of different optical aspects of longitudinal (B, C, D) and transversal (F, G) sections of *Rapana thomasi*, RL, imm, 500X A: Macroscopic rapana shell sections, upper sections prepared for longitudinal visualization of shell layers and the long section prepared for visualization of the transversal shell layers. B: Longitudinal section, amorphous outer shell layer, C: Longitudinal section, intermediate crossed lamellar layer, D: Longitudinal section, inner shell layer or nacre, F: transversal section capturing amorphous outer shell layer, intermediate crossed lamellar layer and nacre. G: transversal section capturing the inner layer of the shell, nacre

The thickness in the middle part of the shell is about  $1380\text{ }\mu\text{m}$ , outer shell layer measuring  $500\text{--}770\text{ }\mu\text{m}$ , intermediate layer about  $170\text{--}215\text{ }\mu\text{m}$  and the inner

layer about 280-400  $\mu\text{m}$ . Depending on the presence/absence of the outer ridges, the thickness is variable. The outer layer is thin near the apex but becomes thicker towards the pallial margin. The inner layer is subdivided into several sublayers (Fig. 1 F, G), and becomes very thin near the growing edge of the shell.

### 3.2. Scanning electron microscopy (SEM)

Transversal and longitudinal sections of the rapana exoskeleton investigated by electron microscopy are presented in Fig. 2.

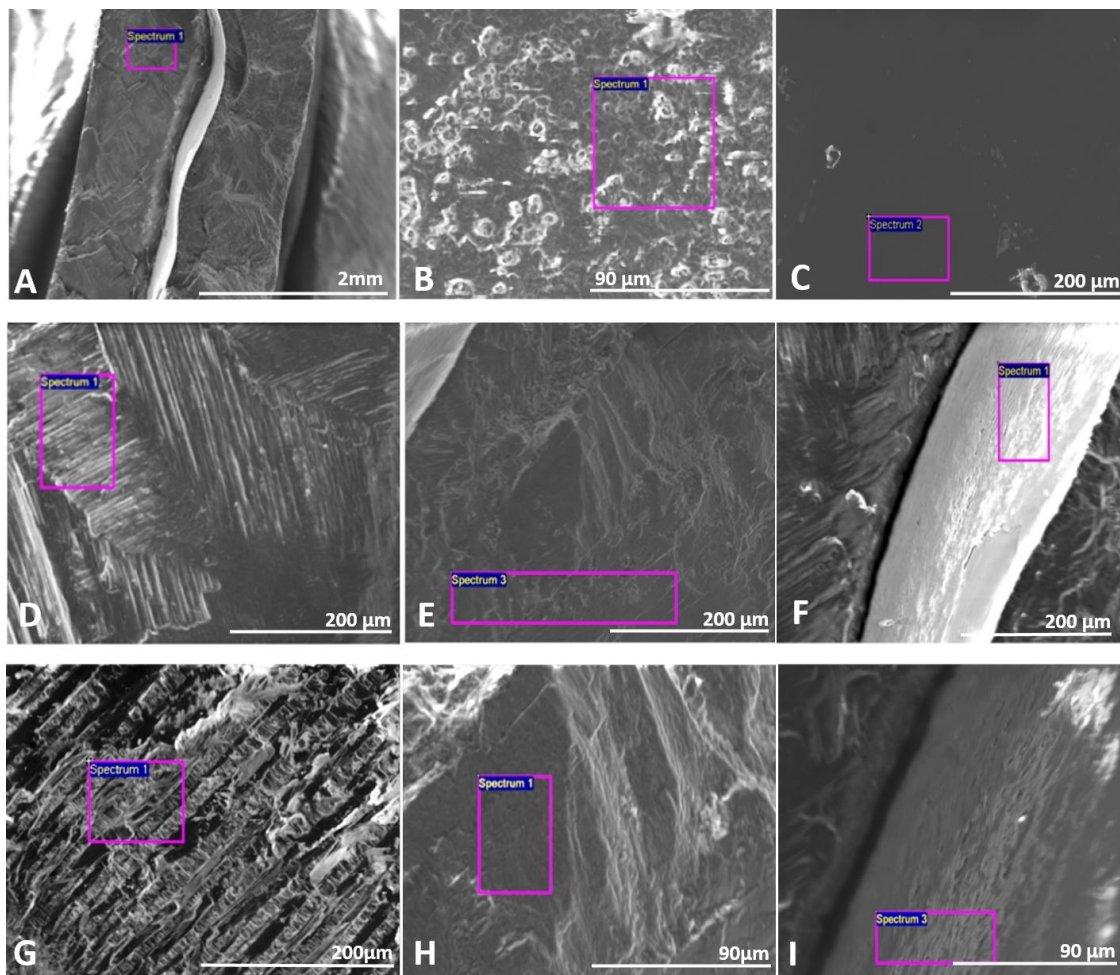


Fig. 2. SEM micrographs of *Rapana thomasiana* - A: Longitudinal section illustrating rapana exoskeletons' main layers, from left to right outer, intermediate and inner shell layer, B: Outer surface of the shell, C: Inner surface of the shell, D: Longitudinal section, inner shell layer or nacre, E, H: Longitudinal section, outer layer of shell, F, I: Longitudinal section, intermediate layer, G: transversal section capturing the inner layer of the shell

Different types of structures found in various layers of rapana shell were determined following the scheme of Hedergaard [15], Carter and Clack [16]. As it was determined by optical microscopy, the shell of *Rapana thomasiana* is well divided in three main layers (Fig. 2 A): an outer, an intermediate and an inner shell layer. No structural characterization could be determined when the outer (Fig. 2 B) or the inner surfaces (Fig. 2 C) of the shell were analysed.

Typically for gastropod shells the inner layer consists of aragonite  $\text{CaCO}_3$  in form of nacre. In the longitudinal section, the inner shell layer of rapana is in form of a regularly foliated layer (Fig. 2 D) and, similarly, visualized in a transversal section presents a lamello-fibrillar structure (Fig. 2 G), meaning that this layer has a laminar structure consisting of sheets of more or less parallel, horizontal rods, with the rods oriented in different directions in adjacent sheets' [16]. Typical columnar nacre could not be observed, but nevertheless rapana nacre is presented in a very complex hierarchical architecture, as long rod shaped aragonite crystals.

The intermediate layer (Fig. 2 F, I), even quite thin, is well separated from the other two main layers. Although at the current magnification it is difficult to characterize the mineral structure of this layer, it seems that a simple prismatic structure can be noticed.

The outer shell layer is formed mainly of crossed lamellar prismatic structures (Fig. 2 E, H) and at the periphery a homogenous  $\text{CaCO}_3$  structure can be noticed. According to other investigations [17, 18], the crossed lamellar prismatic layer consists of calcite  $\text{CaCO}_3$  which contains 1% organic matter, compared with 4,5% in nacre [19].

### 3.3. X-ray fluorescence spectroscopy (XRF)

Three measurements were done for each magnification at 2 mm, 1 mm, 200  $\mu\text{m}$  and 90  $\mu\text{m}$  for the exterior and internal surfaces of the shell, as well as for each of the three main layers of rapana skeleton.

Tables 1 and 2 present the elemental composition for Limanu, respectively Midia Cape samples. Consequently, rapana registered the highest calcium concentration in the outer shell layer with an average of 30%, therefore contains the highest mineral phase consisting of  $\text{CaCO}_3$ , followed by the inner layer with an average of approximately 25%. In the same way, the intermediate layer consists of a higher organic matter since the Ca concentration for this layer is the lowest with an average of 16%, while oxygen concentration is the highest for this shell layer when compared with the other two layers. These results match the observations made by Checa et. al. which have found that outer layer contains 1% organic matter, compared with 4,5% in the inner layer [19].

Furthermore, it can be noticed that traces of Mg, Al, P, Si, S, Cl, K and Sr are present in the *Rapana thomasiiana* shell structure, particularly attached to the outer and inner surface of the exoskeleton.

A comparison between the two sampling locations, Limanu and Midia Cape, regarding rapana shell composition is difficult to make since the XRF beam reveals punctual shell composition.

*Table 1*  
Elemental composition of *Rapana thomasiiana* collected from Limanu

	Outer Surface	Inner Surface	Outer Layer	Intermediate Layer	Inner Layer
Element	Average* (Min – Max)				
	%	%	%	%	%
<b>C</b>	<b>32.40</b> (25.32 - 36.14)	<b>35.87</b> (26.51 - 43.93)	<b>22.12</b> (13.31 - 33.23)	<b>25.68</b> (22.56 - 28.66)	<b>26.23</b> (19.33 - 35.89)
<b>O</b>	<b>44.25</b> (35.26 - 48.16)	<b>48.86</b> (45.98 - 54.32)	<b>47.37</b> (35.74 - 52.84)	<b>57.20</b> (54.67 - 59.35)	<b>51.18</b> (42.94 - 56.92)
<b>Na</b>	<b>0.19</b> (0.01 - 0.37)	<b>0.46</b> (0.26 - 0.67)	<b>0.14</b> (0 - 0.58)	<b>0.29</b> (0 - 0.44)	<b>0.43</b> (0 - 0.76)
<b>Mg</b>	<b>0.22</b> (0.13 - 0.35)	<b>0.14</b> (0 - 0.35)	<b>0.19</b> (0 - 0.6)	<b>0.02</b> (0 - 0.09)	<b>0.04</b> (0 - 0.17)
<b>Al</b>	<b>0.28</b> (0.14 - 0.56)	<b>0.13</b> (0 - 0.25)	<b>0.09</b> (0 - 0.93)	<b>0.03</b> (0 - 0.13)	-
<b>P</b>	-	-	-	<b>0.06</b> (0 - 0.55)	<b>0.01</b> (0 - 0.15)
<b>Si</b>	<b>0.47</b> (0.17 - 0.99)	<b>0.14</b> (0 - 0.30)	<b>0.08</b> (0 - 0.77)	<b>0.02</b> (0 - 0.1)	-
<b>S</b>	<b>0.12</b> (0 - 0.24)	<b>0.11</b> (0 - 0.21)	<b>0.02</b> (0 - 0.19)	<b>0.08</b> (0 - 0.16)	-
<b>Cl</b>	-	-	-	<b>0.02</b> (0 - 0.17)	<b>0.01</b> (0 - 0.17)
<b>K</b>	<b>0.06</b> (0 - 0.26)	<b>0.12</b> (0 - 0.23)	-	-	<b>0.01</b> (0 - 0.12)
<b>Ca</b>	<b>22.01</b> (16.3 - 28.54)	<b>14.11</b> (7.56 - 21.73)	<b>30.00</b> (17.98 - 50.02)	<b>16.55</b> (15.64 - 17.93)	<b>22.10</b> (18.18 - 26.59)
<b>Sr</b>	-	<b>0.07</b> (0 - 0.29)	-	<b>0.06</b> (0 - 0.23)	-

\* arithmetic mean of values registered by XRF analysis at 2mm, 200  $\mu\text{m}$  and 90  $\mu\text{m}$  resolutions

However, results displayed in Tables 1 and 2 suggest that more elements can be found for Limanu sample, this observation being in agreement with a higher sea water salinity in this site comparing with the Northern location, as it will be demonstrated later based on the infrared spectra analysis. For a better comparison between the sampling locations, the obtained data have been corroborated with the chemical analysis of the entire rapana shell composition performed for each sampling site with an inductively coupled plasma

spectrometer [14]. No statistically significant differences in shell inorganic phase composition (Ca, Mg) of rapana individuals were registered.

Table 2

Elemental composition of *Rapana thomasiiana* collected from Midia

	Outer Surface	Inner Surface	Outer Layer	Intermediate Layer	Inner Layer
Element	Average* (Min – Max)				
	%	%	%	%	%
<b>C</b>	<b>22.62</b> (18.44 - 27.02)	<b>21.13</b> (14.75 - 24.37)	<b>17.05</b> (13.06 - 22.7)	<b>13.04</b> (7.82 - 23.43)	<b>21.36</b> (13.06 - 34.77)
<b>O</b>	<b>56.02</b> (52.61 - 58.87)	<b>61.47</b> (52.77 - 65.87)	<b>44.68</b> (32.32 - 48.72)	<b>52.35</b> (41.51 - 62.25)	<b>50.31</b> (41.51 - 54.62)
<b>Na</b>	<b>0.14</b> (0 - 0.42)	-	<b>0.39</b> (0 - 0.8)	<b>0.07</b> (0 - 0.37)	<b>0.31</b> (0 - 0.61)
<b>Mg</b>	<b>0.17</b> (0 - 0.5)	-	<b>0.14</b> (0 - 0.71)	-	-
<b>Al</b>	<b>0.18</b> (0 - 0.55)	-	-	-	-
<b>Si</b>	<b>0.65</b> (0 - 1.17)	-	-	-	-
<b>K</b>	<b>0.09</b> (0 - 0.26)	-	-	<b>0.01</b> (0 - 0.08)	-
<b>P</b>	-	-	<b>0.02</b> (0 - 0.28)	-	-
<b>Ca</b>	<b>20.13</b> (17.89 - 24.55)	<b>17.40</b> (9.76 - 32.47)	<b>30.06</b> (16.2 - 37.13)	<b>17.22</b> (15.84 - 18.97)	<b>28.03</b> (18.03 - 37.13)
<b>Sr</b>	<b>0.62</b> (0.04-0.70)	<b>0.84</b> (0.06-0.96)	-	-	-

\* arithmetic mean of values registered by XRF analysis at 2mm, 200  $\mu\text{m}$  and 90  $\mu\text{m}$  resolutions

### 3.4. Infrared spectroscopy (FTIR)

The infrared spectra of the two sample types are dominated by the inorganic components which mainly consist in calcium carbonate, easily recognized in various rocks by means of very intensive double degenerated band,  $\nu_3$ , ranging between 1430 and 1500  $\text{cm}^{-1}$ . However, FT-IR technique is able to make distinction between its polymorphic phases, as calcite crystallizes in rhombohedral system, while aragonite in monoclinic. Since calcite exhibits a higher symmetry than aragonite, it is characterized by 4 vibration bands, while for aragonite the degeneracy is raised, and usually 6 vibration bands appear. This is the reason why  $\nu_1$  band at around 1080  $\text{cm}^{-1}$  is inactive in IR for calcite (being active in Raman only), while for aragonite it is active both in IR and Raman spectra. The band  $\nu_2$  appears in calcite at 879  $\text{cm}^{-1}$  and in aragonite at 866  $\text{cm}^{-1}$ .

The fourth,  $\nu_4$  band, appears at  $706\text{ cm}^{-1}$  in calcite, and it is double degenerated in aragonite:  $706$  and  $711\text{ cm}^{-1}$ .

Even though the calcite is the stable thermodynamic form, in highly saline media such as marine environment, calcium carbonate is mainly precipitated as aragonite.

The main characteristic bands of the IR spectra of the shells sampled from the two sites are collected in the Table 3.

**Table 3**  
**Assessments of infrared spectra for rapana shells sampled from the two sites,  $\text{cm}^{-1}$**

Midia Cape	Limantu	Assessment
2924	2923	$\nu_{\text{CH}_2}$ asymmetric
2852	2852	$\nu_{\text{CH}_2}$ symmetric
1420-1475	1420-1475	$\nu_3 \text{ CaCO}_3$
1083	1083	$\nu_1$ aragonite
876	876	$\nu_2$ calcite
862	861	$\nu_2$ aragonite
712	713	$\nu_4$ aragonite

The analysis of their assessments reveals that in the two samples both calcite and aragonite phases could be identified in comparable extents. However, a more detailed analysis of FT-IR spectra registered on a restrictive domain ( $650 - 2000\text{ cm}^{-1}$ , Fig. 3) shows that the ratio of relative intensities of  $\nu_2$ :  $I_a/I_c$  is equal to 0.76 for Limantu and 0.63 for Midia Cape.

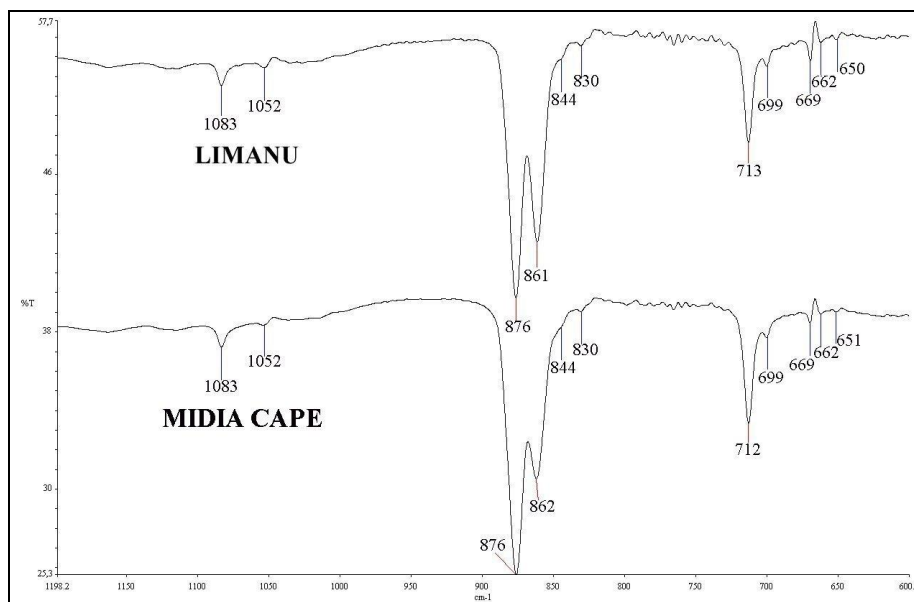


Fig. 3. FT-IR spectra registered for rapana sampled from Limantu (up) and Midia Cape (down)

This indicates a higher relative content in aragonite for Limanu than for Midia Cape, in accordance with the higher salinity in Southern site (15-17 PSU) than in Northern site (11-14 PSU) [20, 21].

Finally, the double band at  $2924-2852\text{ cm}^{-1}$  could be clearly recognized in the high wave number region, even at rather low intensity. This is specific to valence vibration of methylenic groups from organic content, better quantified in elemental analyses data from the *Tables* 1 and 2.

## 6. Conclusions

1. The optical microscopy observations point out that the shell of rapana is characterized by three main layers. These results are confirmed by SEM micrographs in which an amorphous microstructure can be noticed combined with a crossed lamellar prismatic morphology for the outer shell layer, an intermediate simple prismatic layer and a lamello - fibrillar layer for the inner part.
2. Rapana exoskeleton registered the highest mineral phase consisting of  $\text{CaCO}_3$  for the outer shell layer, followed by the inner layer. Among all three shell layers, the intermediate layer consists of the highest organic matter.
3. The FT-IR analysis reveals that in the two samples both calcite and aragonite phases could be identified in comparable extent. However, a higher relative content in aragonite for Limanu than for Midia Cape was registered, results in accordance with the higher water salinity in the Southern site.
4. Traces of Mg, Al, P, Si, S, Cl, K and Sr are present in the shell structure, particularly attached to the outer and inner surfaces of the exoskeleton. Samples from Limanu exhibited more elements than in Midia Cape site, being once again in agreement with the different salinity values of the two sampling sites.

## R E F E R E N C E S

- [1] *R. Mann, A. Occhipinti, and J.-M. Harding, ICES: Alien Species Alert: Rapana venosa (veined whelk), R. Mann, A. Occhipinti, and M.J. Harding, Editors. 2004, International Council for the Exploration of the Sea. p. 14 PP.*
- [2] *V. Zolotarev, The Black Sea Ecosystem Changes Related to the Introduction of New Mollusc Species. Marine Ecology, 1996. **17**(1-3): p. 227-236.*
- [3] *S. Kool, Phylogenetic analysis of the Rapaninae (Neogastropoda: Muricidae) Malacologia 1993 **35**(2 ): p. 155-259.*

[4] *M. Culha, et al.*, Ecology and Distribution of the Veined Rapa Whelk *Rapana venosa* (Valenciennes, 1846) in Sinop Peninsula (Southern Central Black Sea), Turkey. *Journal of Animal and Veterinary Advances*, 2009. **8**(1): p. 51-58.

[5] *M.-T. Gomoiu*, Non-indigenous species in the Romanian Black Sea littoral zone: *Mya arenaria*, *Rapana venosa* and others. *Terre et Environnement*, 2005. **50**: p. 155–176.

[6] *O.B. Boggild*, The shell structure of the mollusks. 1930, Kjobenhavn: A.F. Host.

[7] *M. Petitjean and P. Université de*, Structures microscopiques, nature minéralogique et composition chimique de la coquille des Muricidés, gastéropodes prosobranches : importance systématique de ces caractères, 1965, [s.n.]: [S.l.].

[8] *S. Kiel*, Shell Structures of Selected Gastropods from Hydrothermal Vents and Seeps. *MALACOLOGIA -PHILADELPHIA-*, 2004. **46**: p. 169-184.

[9] *I.P. Bondarev*, Ecomorphological Analyses of Marine Mollusks' Shell Thickness of *Rapana venosa* (VALENCIENNES, 1846)(Gastropoda: Muricidae). *International Journal of Marine Science*, 2013. **3**.

[10] *D.S. M. Castellazzi, A. Occhipinti Ambrogi*, Shell morphotypes of the invasive gastropod *Rapana venosa* in the Northern Adriatic Sea. *Boll. Malacol.*, 2007. **43** p. 103-107.

[11] *D. Savini, et al.*, The alien mollusc "Rapana venosa"(Valenciennes, 1846; Gastropoda, Muricidae) in the Northern Adriatic Sea: Population structure and shell morphology. *Chemistry and Ecology*, 2004. **20**(1): p. 411-424.

[12] *V. Sereanu, M. Mihai, and I. Meghea*, Shell Morphology Of *Rapana thomasiana* Sampled From The Romanian Black Sea Coast, in 14th SGEM GeoConference2014, SGEM2014 Conference Proceedings. p. 531-538.

[13] *O. Jitar, et al.*, Bioaccumulation of heavy metals in marine organisms from the Romanian sector of the Black Sea. *N Biotechnol*, 2015. **32**(3): p. 369-78.

[14] *V. Sereanu, et al.*, Morphology and chemical composition relation of *Rapana thomasiana* shell sampled from the Romanian Coast of the Black Sea. *Continental Shelf Research*, 2016. Available online <http://www.sciencedirect.com/science/article/pii/S0278434316304009>

[15] *C. Hedegaard*, Shell structures of the Recent Vetigastropoda. *JOURNAL OF MOLLUSCAN STUDIES*, 1997. **63**(3): p. 369-378.

[16] *J.G. Carter and G.R. Clark II*, Classification and phylogenetic significance of Molluscan shell microstructure. Broadhead, T. W. (ed.). *Mollusks, Notes for a Short Course*, organized by D. J. Bottjer, C. S. Hickman, and P. D. Ward, University of Tennessee Department of Geological Sciences Studies in Geology 1985 p. 50-71.

[17] *A.B. Rodriguez-Navarro, et al.*, Crystallographic relationships in the crossed lamellar microstructure of the shell of the gastropod *Conus marmoreus*. *Acta Biomater*, 2012. **8**(2): p. 830-5.

[18] *Í. Almagro, et al.*, Crystallography and Textural Aspects of Crossed Lamellar Layers in Arcidae (Bivalvia, Mollusca) Shells. *KEM Key Engineering Materials*, 2016. **672**: p. 60-70.

[19] *A.G. Checa, J.H. Cartwright, and M.G. Willinger*, The key role of the surface membrane in why gastropod nacre grows in towers. *Proc Natl Acad Sci U S A*, 2009. **106**(1): p. 38-43.

[20] *R. The Ministry of Environment and Climate Change*, National Report on the State of Environment in 2014, T.N.E.P. Agency, Editor 2014:  
[http://www.anpm.ro/documents/840114/2987653/RSM\\_APM-C-ta+cf+SOER+2015\\_Final.pdf/9187a3b0-f5e6-49a2-9fb7-4586692a31c4](http://www.anpm.ro/documents/840114/2987653/RSM_APM-C-ta+cf+SOER+2015_Final.pdf/9187a3b0-f5e6-49a2-9fb7-4586692a31c4).

[21] *R. The Ministry of Environment and Climate Change*, National Report on the State of Environment in 2013, T.N.E.P. Agency, Editor 2013:  
<http://www.anpm.ro/documents/12220/2209838/R+S+M+2013+engleza.pdf/daba6dd0-a84b-4973-a14d-e0964d4a0076>. p. 326.